REGIONAL ATTENUATION METHOD COMPARISON FOR NORTHERN CALIFORNIA

Sean R. Ford[1], Douglas S. Dreger[1], Kevin Mayeda[2], William R. Walter[3], Luca Malagnini[4], and William S. Phillips[5]

University of California, Berkeley[1], Weston Geophysical[2], Lawrence Livermore National Laboratory[3], Istituto Nazionale di Geofisca e Vulcanologia[4], Los Alamos National Laboratory[5]

Sponsored by National Nuclear Security Administration
Office of Nonproliferation Research and Development
Office of Defense Nuclear Nonproliferation

Contract No. DE-FC52-05NA26605[1–5]

ABSTRACT

The measurement of regional attenuation (Q^{-1}) is difficult and can produce method dependent results. The discrepancies among methods are due to differing parameterizations (e.g., geometrical spreading considerations), datasets used (e.g., choice of path lengths and sources), and the methodologies themselves (e.g., measurement in the frequency or time domain). This study aims to quantitatively understand differences in regional attenuation measures by applying multiple techniques to common datasets in a several different regions. Here we show results of applying the methods with controlled parameterization in the well-studied region of northern California with a high-quality dataset from the Berkeley Digital Seismic Network. Specifically, we employ the coda normalization, two-station, reverse two-station, source-pair/receiver-pair, and the new coda-source normalization methods to measure Q of the regional phase, Lg (Q_{Lg}), and its power-law dependence on frequency of the form $Q_0 f^{\alpha}$.

All methods produce similar overall regional patterns in Q_0, with low attenuation in the central Sierra Nevada foothills and high attenuation in the Bay Area and northern Sierras. However, the absolute values of Q_0 can differ by as much as a factor of 1.9 for similar paths and stations. The reverse two-station method produces the smallest variance in Q_0, whereas the source-pair/receiver-pair produces the greatest. Spatial variation in α follows that of Q_0, but has more variability for all methods. This variability may be due to the improper accounting of site effects.

We test the sensitivity of each method to changes in geometrical spreading, Lg frequency bandwidth, the distance range of data, and the Lg window. Change in the geometrical spreading model (r^{γ}) affect all methods and is shown to be an important assumption when extracting Q_{Lg} from path effects. There is a significant change in α when measuring Q at frequencies less than 1 Hz, suggesting the power-law frequency dependence of Q may be different at the lower end of the spectrum. All methods are also affected by the choice of the Lg time window, and careful handpicking of the time window may result in less variance in the measurements. Epicentral distance choice has the most effect on the coda-normalization method, which may be due to the fixed elapsed time that the coda is sampled at for all distances. The reverse two-station method is the most robust technique, which is most probably due to its superior suppression of site effects.

OBJECTIVES

Understanding of regional attenuation can help to correct for the effects of *Q* and lead to better discrimination of small nuclear tests. Present threshold algorithms rely on *Q* models that are derived differently, and the models can vary greatly for the same region. For example, recent one-dimensional (1-D) *Q* studies in South Korea find frequency-dependent Q_{Lg} that at 1 Hz range from 450 to 900 (Chung and Lee, 2003; Chung et al., 2005). It is difficult to learn the cause of such discrepancies because the methods and parameterizations change for each analysis. While individual regional attenuation techniques can determine their own self-consistent *Q* parameters, it then becomes a challenge to reconcile new results with other parameterizations in the literature, or to use them in algorithms that may employ different assumptions. These inconsistencies limit the ability to extend prior studies to understand new regions. In order to better understand the effects of different methods and parameterizations on *Q* models, we implement four popular methods and one new method to measure Q_{Lg} with a high-quality dataset from the Berkeley Digital Seismic Network (BDSN). This analysis allows for an "apples-to-apples" comparison of different attenuation methods and their assumptions. With this knowledge, future attenuation studies can more knowledgeably interpret *Q* models.

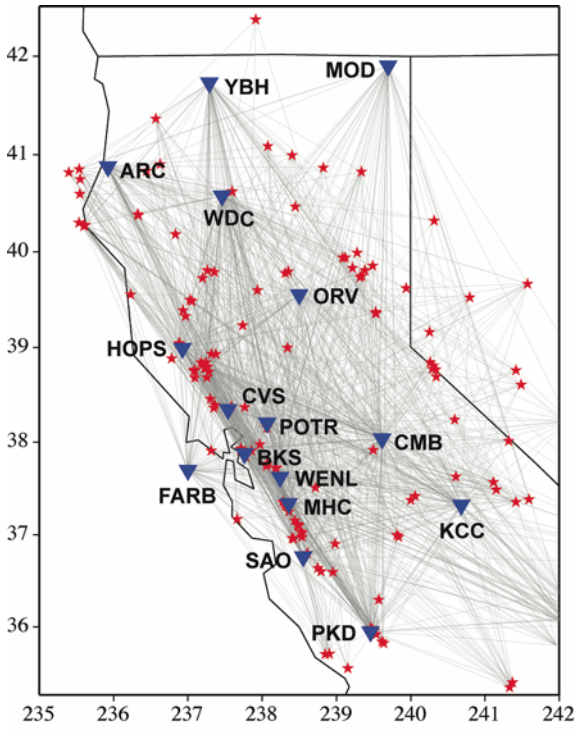

Figure 1. Map of events (red stars), stations (blue inverted triangles), and path coverage (grey lines) employed in this study.

RESEARCH ACCOMPLISHED

The dataset consists of 158 earthquakes recorded at 16 broadband (20 sps) three-component stations of the BDSN between 1992 and 2004 (Figure 1). Records were inspected for a high signal-to-noise ratio and chosen to have a good spatial distribution. Magnitude (mb) ranges from 2.2 to 6.5 (San Simeon event). Distance ranges from 3 to 800 km. Interstation distance ranges from 30 to 670 km. This wide distribution of data parameters allows for sensitivity testing to a given dataset. With this dataset we calculate Q_{Lg} by fitting the power-law model, $Q_0 f^{\alpha}$, in Northern California using five different methods. The first two methods use the seismic coda to correct for the source effect. These methods can produce best-fit power-law parameters for specific stations. The last three methods use the spectral ratio technique to correct for source, and possibly site effects. These methods produce best-fit power-law parameters for specific interstation paths. The two types of methods are briefly introduced and the results compared using the parameterization given in Table 1.

Coda Normalization Method (CNM)

CNM uses the coda as a proxy for the source and removes it from the Lg spectrum (Aki, 1980; Yoshimoto et al., 1993). The amplitude is then least-squares fit as a function of distance in small frequency bands for each station, where the slope is related to path attenuation, Q^{-1}. Q^{-1} at the center frequency of each band then reveals a power-law *Q* model for each station. Results from this method are given in Figure 2a.

Table 1. Method parameterization

Parameter	Value
Lg velocity (km/s)	3.5
Spreading exponent	0.5
Lg velocity window (km/s)	2.5 - 3.5
Component	N-S
Epicentral distance (km)	100 - 400
Measurement bandwidth (Hz)	0.2 - 8
SNR	> 2
Interstation distance (km)	50 - 500
Azimuthal window (°)	15

Coda-source normalization method (CSM)

CSM uses the 1-D coda-source spectra previously calculated in the study by Mayeda et al. (2005) and

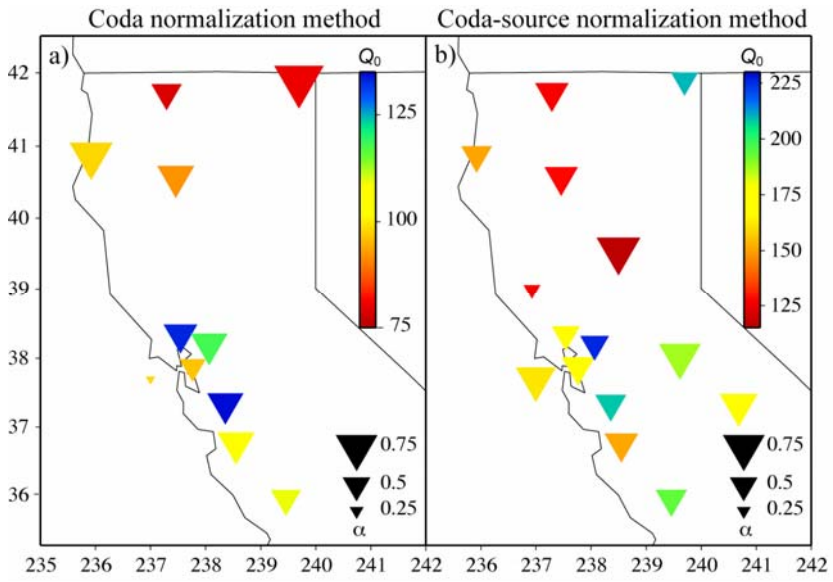

Figure 2. Spatial variability in the power-law fit parameters ($Q_0 f^{\alpha}$) for the coda normalization method (left) and coda-source normalization method (right). Note the similar scales for the parameter α and different scales for Q_0.

removes it from the Lg spectrum in small frequency bands (Walter et al., 2006). Q^{-1} is calculated for each of these bands for each event-station path. In this application of CSM all paths to a common station are fit to find a power-law Q model for each station. Results from this method are given in Figure 2b.

Comparison of CSM and CNM

Since both CNM and CSM give a result for each station, we compare these results by finding the percent deviation

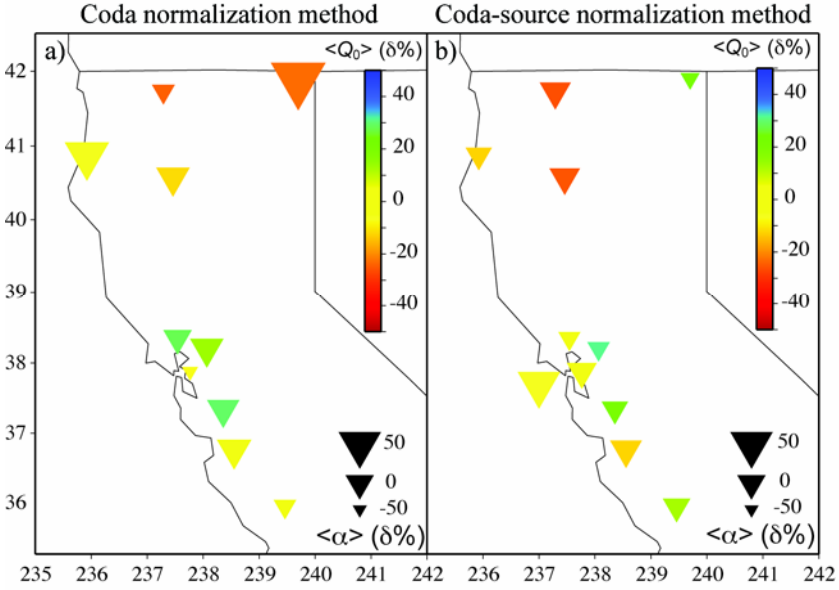

Figure 3. Spatial variability in the percent deviation from the method average power-law fit parameters ($Q_0 f^{\alpha}$) for the coda normalization method (left) and coda-source normalization method (right). The average model ($Q_{Lg} = \langle Q_0 \rangle f^{\langle \alpha \rangle}$) given by CNM is $104 f^{0.61}$ and from CSM is $172 f^{0.57}$.

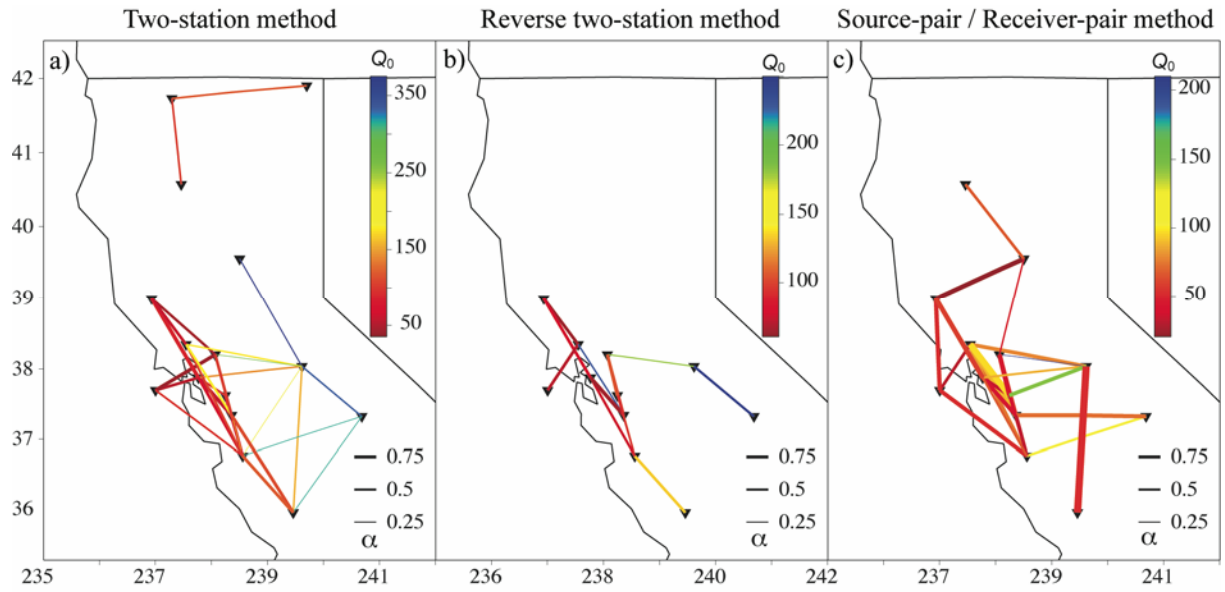

Figure 4. Spatial variability in the power-law fit parameters ($Q_0 f^{\alpha}$) for the three spectral ratio methods. Note the similar scales for the parameter α and different scales for Q_0.

of each station from the average $Q_0 f^{\alpha}$ produced for each method . Comparisons are mapped in Figure 3a-b for robust solutions. The average Q_{Lg} model given by the CNM is $104 f^{0.61}$, while the CSM produces an average of $172 f^{0.57}$. The absolute difference in Q_{Lg} models may be due to the absence of a site correction in the CSM. There is overall relative agreement in the two methods, with low Q in the northern part of the study region and variable Q in the Bay Area. This Bay Area variance may be due to paths crossing different tectonic regimes to reach these stations and forming an average fit. Stations MOD, FARB, and POTR appear to have a strong difference in measured $Q_0 f^{\alpha}$. However, the fit to a power-law model is poor at frequencies > 2 Hz, and the comparison for a power-law model may be flawed for these stations. Stations BKS and MHC are consistently lesser or greater, respectively, than the average for each method, but there is a large percent deviation for the two stations. A possible reason for this deviation may be that the effective SNR is different for the two methods. The signal in the SNR calculation for the CSM is the Lg energy, while the signal for the CNM is the coda. Therefore, it is possible that noisier data is used in the CSM, though this effect would most probably be seen across all stations and not just these two.

Two-Station Method (TSM)

TSM takes the spectral ratio of Lg recorded at two different stations along the same narrow path from an event (Xie, 2002; Xie and Mitchell, 1990). We restricted the path to fall in an azimuthal window of 15°. The ratio removes the common source term and the amplitude is fit in the log domain so that the slope is α and the intercept is Q. Results from this method are given in Figure 4a.

Reverse Two-Station Method (RTSM)

RTSM uses two TSM setups where an event is on either side of the station pair in a narrow azimuthal window (Chun et al., 1987; Fan and Lay, 2003). The two ratios are combined to remove the common source and site terms and the amplitude is fit in the log domain so that the slope is α and the intercept is Q. Results from this method are given in Figure 4b.

Source-Pair / Receiver-Pair Method (SPRPM)

SPRPM is basically the RTSM with a relaxation on the narrow azimuthal window requirement (Shih et al., 1994). Results from this method are given in Figure 4c.

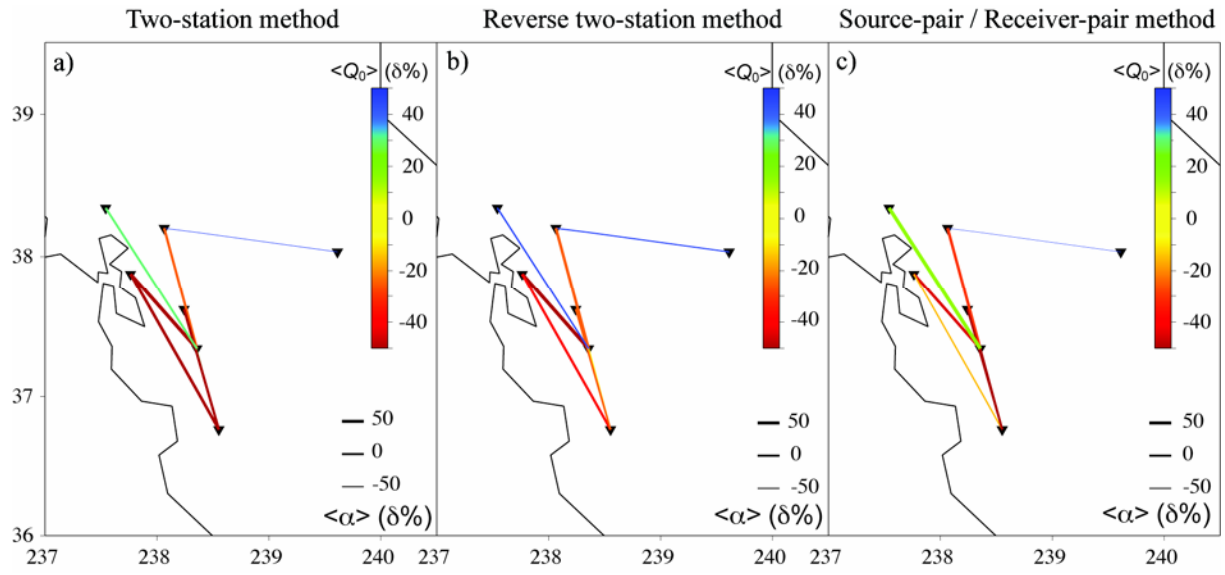

Figure 5. Spatial variability in the percent deviation from the method average power-law fit parameters ($Q_0 f^{\alpha}$) for the three spectral ratio methods. The average model ($Q_{Lg} = \langle Q_0 \rangle f^{\langle \alpha \rangle}$) given by TSM is $132 f^{0.53}$, by RTSM is $121 f^{0.52}$, and by SPRP is $76 f^{0.76}$.

Comparison of TSM, RTSM, and SPRPM

Since TSM, RTSM, and SPRPM give a result for interstation paths, we compare these results by finding the percent deviation of each interstation path from the average $Q_0 f^{\alpha}$ produced for each method. Comparisons are mapped in Figure 4a-c when a solution was calculated for all methods.

The average Q_{Lg} model given by the TSM is $132 f^{0.53}$, by RTSM is $121 f^{0.52}$, and by SPRP is $76 f^{0.76}$. Values of Q_0 are fairly uniform with greater than average and lesser than average consistent across each method. A notable exception is the path from MHC to SAO, where the TSM calculates a greater than average Q_0 and the other methods find a less than average Q_0. There is also a large deviation from mean values for the path from CMB to POTR. The mean value of Q_0 and α for SPRPM are very low for the region. The power-law exponent, α, varies widely among all methods. This may be due to the variance in the spectral amplitudes. More robust methods of spectrum estimation may reduce the variance.

Sensitivity Tests

We investigated how the choice of parameterization affects the results. In each test only one parameter was varied and $Q_0 f^{\alpha}$ was calculated with each of the methods. The varied parameters were geometrical spreading dependence (r^{γ}), measurement bandwidth, epicentral distance of the data, and the Lg window (Table 2). This range of parameterization was

Table 2. Sensitivity test parameterization (varied values in red).

Parameter	Test 1	Test 2	Test 3	Test 4
Lg velocity (km/s)	3.5	3.5	3.5	3.5
Spreading exponent (r^{γ})	0.83	0.5	0.5	0.5
Lg velocity window (km/s)	2.6 - 3.5	2.6 - 3.5	2.6 - 3.5	3.0 - 3.6
Component	Vertical	Vertical	Vertical	Vertical
Epicentral distance (km)	100 - 400	100 - 400	100 - 700	100 - 400
Interstation distance (km)	50 - 500	50 - 500	50 - 500	50 - 500
Measurement bandwidth (Hz)	0.5 - 8	0.25 - 4	0.5 - 8	0.5 - 8
SNR	> 2	> 2	> 2	> 2
Coda critical time (s)	150	150	150	150
Azimuthal window (deg)	15	15	15	15

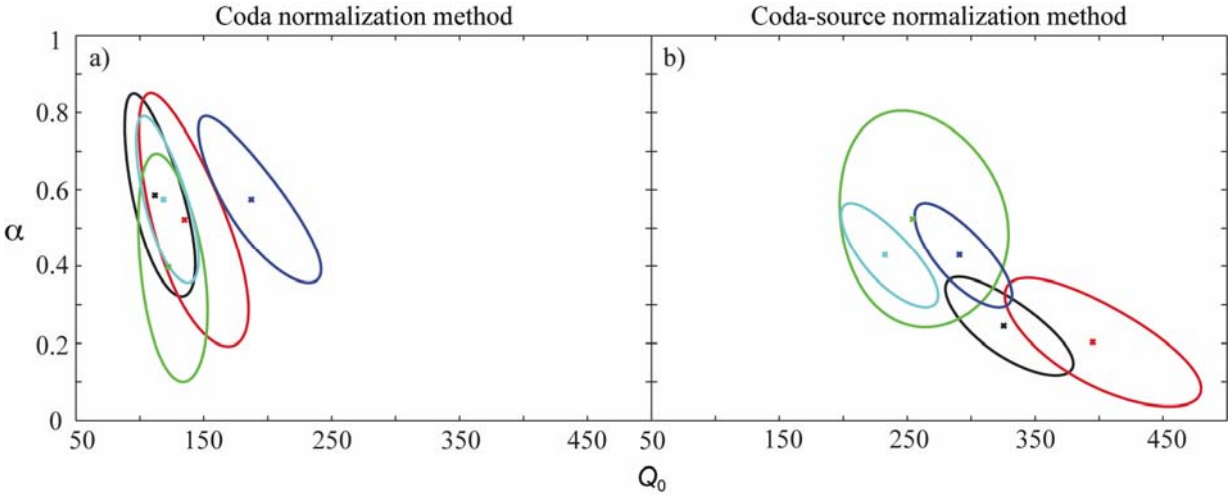

Figure 6. 95% confidence ellipses for the power-law model parameters for station PKD calculated by the coda normalization (left) and coda-source normalization (right) methods obtained by the original parameterization (black), and by varying the spreading exponent (red), bandwidth (green), distance (dark blue), and time window (light blue). The small cross is the best-fitting parameter estimate.

chosen based on the values used in previous studies.

All methods were affected by a change in spreading exponent, where there is a systematic increase in both Q_0 and α as the spreading exponent increases. Also, when more of the spectrum below 1 Hz is sampled, α can change significantly. The methods that use a maximum Lg amplitude in the time domain to measure Q_{Lg}, CNM and SPRP, are less sensitive to Lg window choice than the other methods. However, CNM is affected by epicentral distance, which may be due to the fixed time that the coda is sampled for all distances. The RTSM is the most robust and resistant to changes in parameterization.

In order to better visualize the sensitivity of the methods to varied parameterization, we produce 1-D power-law Q models for a common station, PKD, for the coda-based methods (Figure 6), and a common path, MHC to POTR, for the spectral ratio based methods (Figure 7). Error in these 1-D fits is calculated and we produce 95% confidence ellipses for each of the power-law model parameters (Aster et al., 2005). Figures 6 and 7 allow for an analysis of both the epistemic (model-based) uncertainty due to the relative location of the ellipse and aleatoric (random, data-based) uncertainty due to the size of the ellipse.

Estimates of the power-law parameters, Q_0 and α, have a complex relationship with parameterization choice. The most variance in Q_0 is given by the CSM (~200 - 500), while there is a large variance in α calculated with the SPRPM (~0.6 - 1.8). However, for all methods (with the possible exception of the RTSM) the 95% confidence region is large and the range of the parameter estimates is greater than is given by previous 1-D Q_{Lg} studies, which often only present one choice of parameterization.

CONCLUSIONS AND RECOMMENDATIONS

There is lateral variability in Q_{Lg} at 1 Hz and the power-law dependence on frequency in Northern California. The spatial variability is similar to that found by Mayeda et al. (2005), where there is high attenuation in the northern region of the study area and variable attenuation in the Bay Area. Trends in calculated power-law parameters are similar among the methods investigated in this study, though there is large variability in the absolute values for $Q_{Lg}f^{\alpha}$. The coda-based methods can produce a power-law Q model for each raypath, and though in this study we report station averages, these methods lend themselves more naturally Q tomography. The two station methods are more restrictive in data selection and Q tomography may be difficult in regions without dense station coverage and high seismicity.

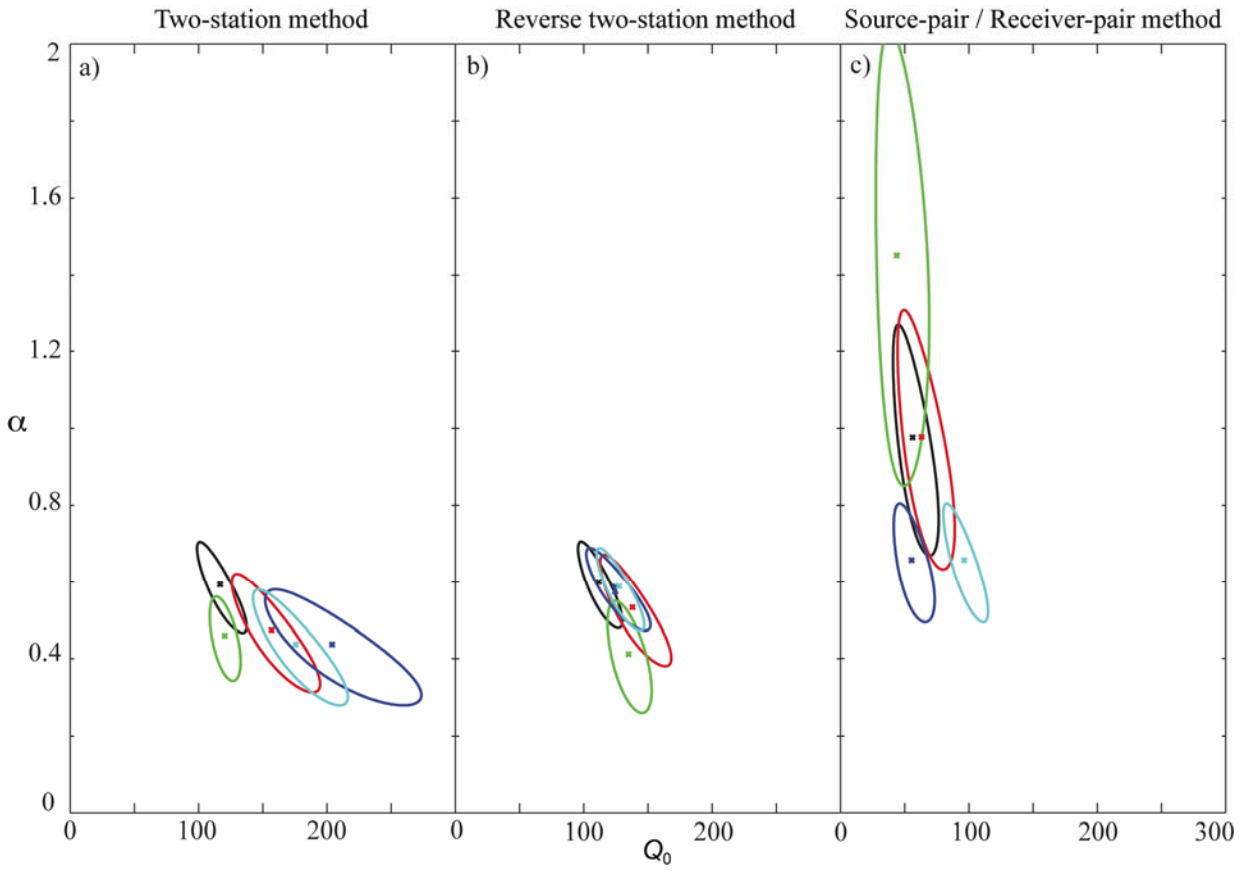

Figure 7. 95% confidence ellipses for the power-law model parameters for the path MHC to POTR calculated by (a) the TSM (b) the RTSM, and (c) the SPRPM obtained by the original parameterization (black), and by varying the spreading exponent (red), bandwidth (green), distance (dark blue), and time window (light blue). The small cross is the best-fitting parameter estimate.

The choice of spreading exponent, distance, and measurement window has a large influence on the best-fit power-law parameter estimates. Unless the parameterization choice can be constrained from a priori information, regional attenuation studies should search the entire solution space in order to report useful power-law *Q* models.

REFERENCES

Aki, K. (1980). Attenuation Of Shear-Waves In The Lithosphere For Frequencies From 0.05 To 25 Hz, *Phys. Earth Planet. Inter.*, 21: 50–60.

Aster, R. C., and B. Borchers, and C. H. Thurber (2005). *Parameter Estimation and Inverse Problems*. San Diego: Elsevier Academic Press.

Chun, K. Y., G. F. West, R. J. Kokoski, and C. Samson (1987). A Novel Technique For Measuring Lg Attenuation - Results From Eastern Canada Between 1-Hz To 10-Hz, *Bull Seism Soc.* 77: 398–419.

Chung, T. W., and K. W. Lee (2003). A study of high-frequency Q(Lg)(-1) in the crust of South Korea, *Bull Seism Soc.* 93: 1401–1406.

Chung, T. W., Y. K. Park, I. B. Kang, and K. Lee (2005). Crustal Q(Lg)(-1) in South Korea using the source pair/receiver pair method, *Bull Seism Soc.* 95: 512–520.

Fan, G. W., and T. Lay (2003). Strong Lg wave attenuation in the Northern and Eastern Tibetan Plateau measured by a two-station/two-event stacking method, *Geophys. Res. Lett.* 30.

Mayeda, K., L. Malagnini, W. S. Phillips, W. R. Walter, and D. Dreger (2005). 2-D or not 2-D, that is the question: A northern California test, *Geophys. Res. Lett.* 32.

Shih, X. R., K. Y. Chun, and T. Zhu (1994). Attenuation Of 1-6-S-L(G) Waves In Eurasia, *J. Geophys. Res.* 99: 23859–23873.

Walter, W. R., K. Mayeda, L. Malagnini, L. Scognamiglio (2006). Regional body-wave attenuation using a coda source normalization method: application to MEDNET records of earthquake in central Italy, *Seism. Res. Lett.* 77: 260.

Xie, J. K. (2002). Lg Q in the eastern Tibetan Plateau, *Bull Seism Soc.*, 92: 871–876.

Xie, J., and B. J. Mitchell (1990). Attenuation Of Multiphase Surface-Waves In The Basin And Range Province.1. Lg And Lg Coda, *Geophys. J. Int.* 102: 121–137.

Yoshimoto, K., H. Sato, and M. Ohtake (1993). Frequency-Dependent Attenuation Of P-Wave And S-Wave In The Kanto Area, Japan, Based On The Coda-Normalization Method, *Geophys. J. Int.* 114: 165–174.